P-glycoprotein (*ABCB1*) activity decreases raltegravir disposition in primary CD4+P-gp^{high} cells and correlates with HIV-1 viral load

Gerard Minuesa[1]†, Cristina Arimany-Nardi[2,3], Itziar Erkizia[1], Samandhy Cedeño[1], José Moltó[4],
Bonaventura Clotet[1,4,5], Marçal Pastor-Anglada[2,3] and Javier Martinez-Picado[1,5,6]*

[1]AIDS Research Institute IrsiCaixa, Institut d'Investigació en Ciències de la Salut Germans Trias i Pujol, Universitat Autònoma de Barcelona, Badalona, Spain; [2]Molecular Pharmacology and Experimental Therapeutics, Department of Biochemistry and Molecular Biology, Institute of Biomedicine (IBUB), University of Barcelona, 08028 Barcelona, Spain; [3]Oncology Program, National Biomedical Research Institute on Liver and Gastrointestinal Diseases (CIBER EHD), Instituto de Salud Carlos III, Madrid, Spain; [4]Fundació Lluita contra la Sida, Hospital Universitari Germans Trias i Pujol, Badalona, Spain; [5]Institució Catalana de Recerca i Estudis Avançats (ICREA), Barcelona, Spain; [6]Universitat de Vic, Universitat Central de Catalunya (UVic-UCC), Vic, Spain

*Corresponding author. E-mail: jmpicado@irsicaixa.es
†Present address: Molecular Pharmacology Program, Experimental Therapeutics Center and Center for Cell Engineering, Memorial Sloan-Kettering Cancer Center, New York, NY, USA.

Objectives: To evaluate the role of P-glycoprotein (P-gp) and multidrug-resistant-protein 1 (MRP1) on raltegravir intracellular drug disposition in CD4+ T cells, investigate the effect of HIV-1 infection on P-gp expression and correlate HIV-1 viraemia with P-gp activity in primary CD4+ T cell subsets.

Methods: The cellular accumulation ratio of [3H]raltegravir was quantified in CD4+ T cell lines overexpressing either P-gp (CEM-P-gp) or MRP1 (CEM-MRP1) and in primary CD3+CD4+ T cells with high (P-gp^{high}) and low P-gp activity (P-gp^{low}); inhibition of efflux transporters was confirmed by the intracellular retention of calcein-AM. The correlation of P-gp activity with HIV-1 viraemia was assessed in naive and memory T cell subsets from 21 HIV-1-infected treatment-naive subjects.

Results: [3H]Raltegravir cellular accumulation ratio decreased in CEM-P-gp cells (*P* < 0.0001). XR9051 (a P-gp inhibitor) and HIV-1 PIs reversed this phenomenon. Primary CD4+P-gp^{high} cells accumulated less raltegravir (38.4% ± 9.6%) than P-gp^{low} cells, whereas XR9051 also reversed this effect. *In vitro* HIV-1 infection of PBMCs and stimulation of CD4+ T cells increased P-gp mRNA and P-gp activity, respectively, while primary CD4+P-gp^{high} T cells sustained a higher HIV-1 replication than P-gp^{low} cells. A significant correlation between HIV-1 viraemia and P-gp activity was found in different CD4+ T cell subsets, particularly memory CD4+ T cells (*r* = 0.792, *P* < 0.0001).

Conclusions: Raltegravir is a substrate of P-gp in CD4+ T cells. Primary CD4+P-gp^{high} T cells eliminate intracellular raltegravir more readily than P-gp^{low} cells and HIV-1 viraemia correlates with P-gp overall activity. Specific CD4+P-gp^{high} T cell subsets could facilitate the persistence of viral replication *in vivo* and ultimately promote the appearance of drug resistance.

Introduction

Raltegravir, the first HIV-1 integrase inhibitor (INI) approved by the FDA in 2007, is a key component of HAART in the treatment of HIV-1 infection.[1] Even though raltegravir-containing HAART has been mostly associated with favourable clinical and virological outcomes,[2–8] treatment failure still occurs.[9] Raltegravir needs to cross the plasma membrane to get into the cytoplasm of HIV-1-infected cells to block viral integration efficiently. Thus, its drug efficacy represents the interplay between cellular entry and efflux processes.[10–12] It is crucial to understand the efflux mechanisms that occur in T lymphocytes and other cells susceptible to HIV-1 infection as they could be responsible for elimination of the drug, limiting its intracellular concentration, and favouring the emergence of resistant viruses and subsequent HIV-1 therapy failure.[13] Moreover, this efflux transporter activity could influence the suboptimal penetrance of drugs into viral sanctuaries[14] and the complete elimination of HIV-1 reservoirs in the body.

Initial pharmacological studies of raltegravir showed a complex pharmacokinetic/pharmacodynamic relationship.[4] However, sustained plasma levels of raltegravir (above IC$_{95}$), particularly at the end of the dosing interval, are crucial for an optimal clinical response.[15–17] *In vitro* studies have shown that the drug has a 'post-antibiotic' effect,[18] which could be associated with low levels of efflux transport in specific immune cell subsets. Interestingly, raltegravir shows a low cellular penetration (~5% of blood cells) and its cellular disposition is highly variable between patients (giving up to 15-fold difference)[19] and within same patients after consecutive evaluations.[20] Furthermore, the specific effect of antiviral drugs with known inhibitory activity of efflux transporters (i.e. ritonavir) in different CD4+ T cell subsets has never been addressed.

The best-known efflux pumps of the ATP-binding cassette (ABC) superfamily of transporters are P-glycoprotein (P-gp; *ABCB1*, also known as *MDR1*) and multidrug resistance related-protein 1 (MRP1; *ABCC1*). Both have been shown to be involved in the efflux of HIV-1 PIs[21–23] and whereas NNRTIs do not seem to be substrates for P-gp, MRP1 could influence their drug disposition in T cells.[24] This efflux function can compromise optimal intracellular drug concentrations[25,26] with potential consequences in drug resistance and/or viral persistence. To date, only few studies have specifically addressed the question of how HIV-1 INI are extruded from cells and have been mostly focused on either CD4+ T cell lines, blood–tissue barriers or gastrointestinal model systems.[13,27–30]

Herein, we aimed to evaluate the role of P-gp and MRP1 on raltegravir intracellular drug disposition in CD4+ T cells, to investigate the effect of cell activation and HIV-1 infection on P-gp expression, and to correlate HIV-1 viral load with P-gp activity in primary CD4+ T cell subsets.

Materials and methods

Reagents

The reagents used in uptake and inhibition experiments were raltegravir and [^{3}H]raltegravir (41 Ci/mmol; 0.53 mCi/mL) (Merck, USA) and [^{3}H]ritonavir (25.2 Ci/mmol; 1 mCi/mL) (Hartmann Analytics, Germany), MK571 (MRP1 inhibitor) (Sigma-Aldrich, St Louis, MO, USA), reversan (MRP1 and P-gp inhibitor), XR9051 and Ko143 [inhibitor of BCRP (ABCG2) at <1 μM and of MRP1 and P-gp at >1 μM] (Tocris Biosciences, Bristol, UK) and the fluorescent dyes calcein-AM and rhodamine-123 (Rho123) (Invitrogen, Paisley, UK). PIs and NNRTIs were obtained through the AIDS Research and Reference Reagent Program (NIAID, NIH, USA). The remaining reagents were purchased from Sigma-Aldrich unless indicated in the text.

Cell culture

The model CD4+ T lymphoblastoid cell lines CEM-CCRF (WT), CEM$_{E1000}$ [MRP1 (*ABCC1* gene) overexpressing] and CEM$_{VBL100}$ [P-gp (*ABCB1* gene) overexpressing] were kindly provided by Prof Dr Ross Davey (Bill Walsh Cancer Research Laboratories, Royal North Shore Hospital, Sydney, Australia). CEM$_{E1000}$ cells had been previously obtained by stepwise selection with epirubicin to a final concentration of 1 μg/mL and CEM$_{VBL100}$ were selected with vinblastine to a final concentration of 100 ng/mL.[31,32] All CEM cells were routinely cultured in RPMI 1640 culture medium supplemented with 10% heat-inactivated FBS, 2 mM L-glutamine and 100 U/mL penicillin and 100 μg/mL streptomycin (Gibco BRL; Paisley, Scotland), and maintained at 37°C in a humidified atmosphere containing 5% CO$_2$. Three or four days prior to use in radiotracer and/or fluorescence substrate(s) accumulation experiments, cells were stained with specific antibodies (anti-MRP1 PE-labelled and anti-P-gp PE-labelled; BD Biosciences)

to ensure that they showed the correspondent phenotype (Figure S1a, available as Supplementary data at *JAC* Online). Routinely, cells were cultured at 0.5×10^6 cells/mL concentration the day before using them.

PBMCs were isolated from HIV-1-seronegative donors by Ficoll-Hypaque density gradient centrifugation of heparin-treated venous blood. Cells were stimulated for 3 days by adding 3 μg/mL phytohaemagglutinin (PHA; Invitrogen, Paisley, Scotland) and 10 IU/mL IL-2 (Roche, Basel, Switzerland). All primary cells were maintained in RPMI 1640 supplemented with 2 mM L-glutamine, 20% FBS and 100 U/mL penicillin and 100 μg/mL streptomycin (Gibco BRL).

Primary blood cells from human donors and HIV-1 patients

PBMCs were obtained from healthy human volunteers and HIV-1-infected subjects by Ficoll-Hypaque density gradient centrifugation. The study included cryopreserved PBMCs from 21 HIV-1-infected treatment-naive subjects. Median plasma HIV-1 RNA was 4.5 log$_{10}$ copies/mL (IQR=4.1–5.3), median CD4+ T cell count was 630 cells/mm^3 (IQR=411–780) and median CD8 T cell count was 1104 cells/mm^3 (IQR=883–1371).

Ethics

The institutional review board on biomedical research from Hospital Germans Trias i Pujol (HUGTIP) approved this study (ref. CEI PI-15-154). All patients involved in this study gave their written informed consent to participate. The data were fully anonymized in adherence to the Helsinki Declaration.

Sorting of CD3+CD4+P-gp^{high} and P-gp^{low} T cells

PBMCs were isolated from HIV-1-seronegative donors as described and were resuspended in RPMI 1640 (FBS-free medium) at 30×10^6 cells/mL and incubated for 20 min at 37°C with the P-gp fluorescent substrate Rho123 (Invitrogen, Madrid, Spain) at a final concentration of 1 μM. After the incubation, cells were washed twice in RPMI and cultured in complete medium (RPMI 1640 supplemented with 2 mM L-glutamine, 10% FBS and 100 U/mL penicillin and 100 μg/mL streptomycin) for 2 h to let the fluorescent dye (Rho123) be effluxed by P-gp. Cells were stained with anti-CD3-APC and anti-CD4-PerCP antibodies (BD Biosciences) for 20 min at 4°C in PBS with 1% FBS. After washing, cells were resuspended at 60–80×10^6 cells/mL with PBS plus 1% FBS for cellular sorting. The two cell populations of interest were sorted by FACS Aria II based on their staining in CD3-APC, CD4-PerCP, Rho123; very low Rho123 staining corresponded to CD3+CD4+P-gp^{high}, whereas high Rho123 staining to CD3+CD4+P-gp^{low}. The proportion of CD3+CD4+P-gp^{high} and P-gp^{low} populations varied a lot from donor to donor, but had an average ± SD of 15.7% ± 6.2% and 81.3% ± 7.1%, respectively.

In vitro infection of PBMCs with HIV-1

Four different donors' PBMCs were pooled and cultured in 10 IU/mL IL-2 alone or in combination with 3 μg/mL PHA during 3 days and then infected (10×10^6 cells) with HIV-1$_{NL4-3}$ (CXCR4-tropic strain) at moi of 0.01 and 0.1 during 4 h at 37°C. The excess of virus was washed twice with RPMI complete medium and cells were cultured during 48 h in complete medium. After this period, 5×10^6 cell pellets were washed twice in cold 1× PBS and dry frozen at −80°C until RNA extraction was performed.

Quantitative real-time RT–PCR analysis

Total RNA was isolated from *in vitro* HIV-1-infected PBMCs using RNeasy Mini Kit (Qiagen, Barcelona, Spain). RNA was treated with DNase I from RNase-Free DNase Set (Qiagen) to eliminate contaminating DNA. In total, 1 μg of RNA was retrotranscribed to cDNA using the TaqMan reverse transcription reagents (including Multiscribe reverse transcriptase

and random hexamers) as described by the manufacturer (Applied Biosystems, Foster City, CA, USA). Quantitative real-time PCR was conducted using pre-made TaqMan probes (Applied Biosystems) (00184500_m1, P-gp, *ABCB1*; 14310884E, glyceraldehyde-3-phosphate dehydrogenase, *GAPDH*) in a ABI Prism 7700 sequence detection system (Applied Biosystems) and $\Delta\Delta C_t$ method was applied to obtain a relative quantification of the mRNA levels, according to the TaqMan user's manual and as previously described.[30] GAPDH was used as the housekeeping gene.

Intracellular accumulation ratio experiments with radiolabelled raltegravir and ritonavir

The transport and accumulation of [³H]raltegravir (1 µM, 1 µCi/mL) or 1 µM [³H]ritonavir (1 µM, 1 µCi/mL) was measured by incubating CEM, CEM-MRP1 and CEM-P-gp cells in a final volume of 500 µL of transport medium (137 mM choline chloride plus 5.4 mM KCl, 1.8 mM CaCl₂, 1.2 mM MgSO₄ and 10 mM HEPES, pH 7.4) at 37°C (in a water bath) for 30 min in the absence or presence of fixed concentrations of the following inhibitors: XR9051 (10 µM, P-gp inhibitor), MK571 (100 µM, MRP1 inhibitor), reversan (10 µM, MRP1 and P-gp inhibitor) and/or Ko143 (inhibitor of BCRP, MRP1 and P-gp at >1 µM). We also used the PIs saquinavir and ritonavir, and cold (non-radiolabelled) raltegravir as *cis* inhibitors at 100 µM. Similarly, for primary PBMCs, sorted CD3+CD4+, CD3+CD4+P-gp^high or CD3+CD4+P-gp^low cells were incubated for 30 min at 37°C in transport medium containing [³H]raltegravir (1 µM, 1 µCi/mL) and in the absence or presence of XR9051 (1 µM). After incubation, samples were centrifuged at 12000 rpm for 2 min at 4°C. A 200 µL aliquot of the medium was taken for scintillation counting and the pellets were washed three times in ice-cold PBS before solubilization for radioactivity counting. Data were expressed as the cellular accumulation ratio (CAR) as previously reported.[33]

Calcein accumulation assays in flow cytometry and fluorescence microscopy: inhibition with specific inhibitors and antiviral drugs

To determine the inhibitory potency of a panel of anti-HIV-1 drugs to P-gp/MRP1 efflux activity (raltegravir, PIs and NNRTIs) we performed calcein-AM fluorescence accumulation assays. The method is based on the dye calcein as a substrate for ABC efflux pumps MRP1 and P-gp.[34]

CEM-CCRF cells and its ABC overexpressing variants (0.25×10^6 CEM cells/well in V bottom 96-well plates for flow cytometry experiments; 0.75×10^6 CEM cells/well in 48-well plates for fluorescence microscopy analysis) were incubated in the absence (control) or presence of inhibitors (different concentrations depending on the drug/assay) or antiviral drugs (at 100 µM) and calcein-AM (0.25 µM final concentration) at the same time. Following 30 min of incubation at 37°C, the cells were centrifuged (1400 rpm, 5 min) and washed twice in ice-cold PBS plus 1% FBS. Finally, cells were fixed with 100 µL ice-cold 1% paraformaldehyde solution in PBS and the cell preparations for fluorescence microscopy were mounted on to poly-L-lysine pretreated glass slides. The calcein fluorescence was monitored by an LSRII flow cytometer (Becton Dickinson). Cells were also evaluated in a fluorescence microscope Nikon Eclipse TE200.

Immunophenotype staining of HIV-1-seronegative blood donors and HIV-1-infected subjects

To characterize the HIV-1 co-receptors surface expression and to establish correlation of different subsets of CD3+CD4+ T cells with P-gp activity, we used two different panels of antibodies and Rho123 as P-gp fluorescent substrate. After isolating the PBMCs from HIV-1-seronegative donors and HIV-1-infected subjects, cells were resuspended in RPMI 1640 and stained with Rho123 as described in the previous section. Cells were then stained with two panels of antibodies: (i) Rho123 (FL1 channel), anti-CD4-APC, anti-CXCR4-PE, anti-CCR5-PerCP-Cy5.5 and anti-CD3-APC-Cy7 (all from Becton Dickinson); and (ii) anti-CD4-APC, anti-CCR7-PerCP-Cy5.5, anti-CD45RA-PE-Cy7, anti-CD27-V450/Pacific Blue and anti-CD3-APC-Cy7 (Becton Dickinson). After washing the excess of antibodies, cells were run on a LSRII flow cytometer (Becton Dickinson) and results analysed by FlowJo Software (vX.0.7) and GraphPad Prism 6. Statistical analysis for each staining and graph are detailed in the figure legends.

Results

[³H]Raltegravir time-course and CAR in CEM cells

First, we performed time-course experiments of [³H]raltegravir in our CD4+ T cell model cell lines (CEM-WT and CEM-P-gp cells) to
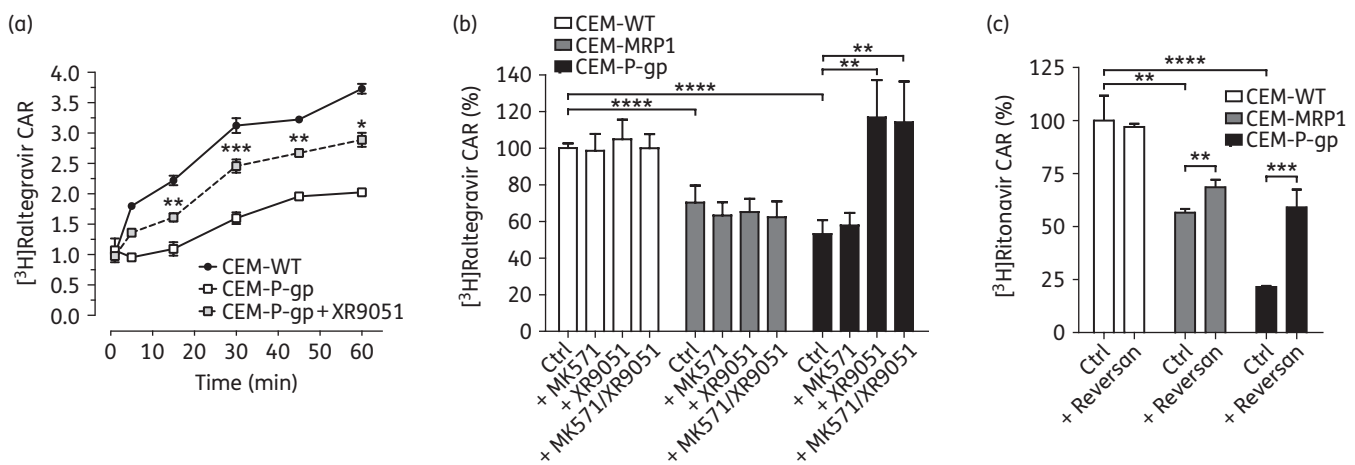

Figure 1. Time-course and inhibition of [³H]raltegravir efflux in CEM cells. (a) [³H]Raltegravir (1 µM; 0.5 µCi/mL) CAR was performed at different time points (1, 5, 15, 30, 45 and 60 min) in CEM-WT and CEM-P-gp in the absence and presence of 1 µM of the P-gp inhibitor XR9051. (b) CAR (%, normalized to CEM-WT, control cells) at 30 min was assessed in CEM-WT, CEM-MRP1 and CEM-P-gp in the absence (control) and presence of MRP1-specific (MK571) and P-gp-specific (XR9051) inhibitors. (c) [³H]Ritonavir (1 µM; 1 µCi/mL) CAR (%, normalized to CEM-WT, control) was performed in the same cells in the absence (control) or presence of the MRP1/P-gp dual inhibitor reversan. The results represent the mean ± SEM of at least three independent experiments in duplicate. Statistical significance between control in CEM-WT, CEM-MRP1 or CEM-P-gp and between control and treatment in CEM-MRP1 and P-gp was assessed by paired *t*-test (*P<0.05; **P<0.01; ***P<0.001; ****P<0.0001). Ctrl, control.

confirm the role of P-gp in raltegravir efflux. As shown in Figure 1(a), the CAR of raltegravir (a direct measure of intracellular accumulation of the drug) was significantly higher in CEM-WT cells than in CEM-P-gp cells at any time chosen (i.e. 3.12 ± 0.12 versus 1.59 ± 0.96 at 30 min). Most importantly, when co-incubating the CEM-P-gp cells with XR9051 (1 μM), a highly potent and specific inhibitor of P-gp activity, the intracellular accumulation of [^{3}H]raltegravir significantly increased, the effect being more remarkable at longer incubation times (i.e. 1.59 ± 0.10 versus 2.46 ± 0.10, $P=0.0025$ at 30 min). The same treatment with XR9051 on CEM-WT did not significantly alter [^{3}H]raltegravir CAR (data not shown). In addition, after re-confirming overexpression of MRP1 and P-gp by flow cytometry (Figure S1a) we investigated the cellular uptake of raltegravir at short time points (up to 5 min). We found that the linearity of the uptake (associated exclusively with influx transporters) was very short, particularly in CEM-P-gp cells (Figure S1b) and remarkably, up to 1 min, the uptake of both cell lines was very similar (see insert). At longer time points, the notable differences in raltegravir intracellular levels were mostly due to higher raltegravir efflux via P-gp.

In raltegravir accumulation experiments at 30 min (Figure 1b), the CAR of raltegravir in CEM-WT was 3.04 ± 0.62 (normalized to 100% for relative comparisons). The treatment with the MRP1-specific (MK571) and P-gp-specific (XR9051) inhibitors, either alone or in combination, did not affect the drug accumulation ratio in these cells. For CEM-MRP1 cells we found a reduction in intracellular raltegravir accumulation of >30% in untreated cells (control) with respect to control CEM-WT cells (CAR raltegravir$_{MRP1}$/CAR raltegravir$_{WT}=0.64$, $P<0.0001$), but neither MK571 nor XR9051 affected raltegravir accumulation. In CEM-P-gp cells, in contrast, the effect of P-gp function in raltegravir efflux was clear; while untreated cells (control) showed a significant 52% reduction with respect to CEM-WT (CAR raltegravir$_{P-gp}$/CAR raltegravir$_{WT}=0.48$, $P<0.0001$), the presence of XR9051 significantly increased accumulation of raltegravir, either alone ($P=0.0017$) or in combination with MK571 ($P=0.0077$). This demonstrates the involvement of P-gp in raltegravir efflux in T lymphocytes.

The HIV-1 PIs, saquinavir and ritonavir, are known substrates and inhibitors of both MRP1 and P-gp *in vitro* and *in vivo*.[35,36] Thus, as a positive control of our experimental approach and of optimal MRP1 and P-gp activity in CEM cells, we performed intracellular accumulation experiments with the PI ritonavir (Figure 1c). As found for raltegravir, ritonavir accumulation was higher in control CEM-WT cells than in CEM-MRP1 ($P=0.015$) or CEM-P-gp cells ($P<0.0001$). Of note, reversan (an inhibitor of both MRP1 and P-gp) reversed in part this phenomenon in MRP1 ($P=0.037$) and P-gp overexpressing cells ($P=0.0021$).

In conclusion, raltegravir intracellular accumulation depends on P-gp as demonstrated by CD4+ T lymphoblastoid CEM P-gp overexpressing cells. MRP1 does not significantly contribute to raltegravir cellular efflux.

Raltegravir in vitro drug−drug interaction(s) with PIs

After demonstrating that ritonavir is a good substrate of both MRP1 and P-gp in our system, we tested whether we could inhibit raltegravir efflux through these ABC transporters in CEM cells by competing in the presence of ritonavir or saquinavir (Figure 2a). As for the specific inhibitors, both PIs significantly competed with raltegravir efflux in CEM-P-gp cells (saquinavir, $P<0.0001$;

ritonavir, $P=0.0001$), whereas they did not affect raltegravir intracellular accumulation in CEM-WT or CEM-MRP1. Interestingly, in the presence of 100 μM cold raltegravir we found no changes in [^{3}H]raltegravir accumulation neither in CEM-WT, CEM-MRP1 nor in CEM-P-gp. This result demonstrates that, even though being a substrate, raltegravir itself is not an inhibitor of MRP1 or P-gp function either because, by competing with the cold drug, we did not reach saturating concentrations, or it is not an allosteric inhibitor.

Using PIs as control substrates (Figure 2b), we performed [^{3}H]ritonavir (1 μM) CAR experiments in the presence of 100 μM cold saquinavir, ritonavir and raltegravir. In CEM-MRP1, only cold ritonavir was capable of significantly increasing the CAR of [^{3}H]ritonavir by 25% ($P<0.005$). In CEM-P-gp cells, both saquinavir and ritonavir significantly increased the CAR of ritonavir (by 30% for saquinavir and 60% for ritonavir, $P<0.005$ and $P<0.001$). Cold raltegravir did not inhibit MRP1 or P-gp activity in CEM-MRP1 or CEM-P-gp, as previously suggested elsewhere[30] either using [^{3}H]raltegravir or [^{3}H]ritonavir as a substrate.

Using a fluorescence-based assay in CEM-WT and CEM-P-gp cells, we found a clearly reduced calcein accumulation in P-gp overexpressing cells compared with CEM-WT (Figure 2c). Of note, we could reverse this effect by using verapamil (a broad-spectrum ABC transporter inhibitor) and ritonavir, but not raltegravir. Assessing the fluorescence by flow cytometry, we tested the inhibition potency of different efflux transporter inhibitors, as well as a battery of HIV-1 PIs. The P-gp-specific XR9051 (1 μM), the broad-spectrum verapamil (20 μM) and Ko143 (50 μM) were the best inhibitors of P-gp function (see MFI [calcein]$_{P-gp}$/[calcein]$_{WT}$ in Table 1 and histograms in Figure S2). The MRP1-specific inhibitor MK571 did not alter the accumulation in CEM-P-gp, whereas it did affect, although slightly, the accumulation of calcein in CEM-MRP1 (Table 1). Among the PIs tested, amprenavir, atazanavir, lopinavir, ritonavir and saquinavir (but not indinavir, which only inhibited MRP1, although to a lesser extent) affected calcein accumulation in both MRP1 and P-gp overexpressing cells significantly increasing the intracellular fluorescent signal (Table 1 and Figure S2). Regarding NNRTIs, only efavirenz inhibited MRP1 and P-gp function showing a 4.9-fold higher effect in P-gp cells (Table 1). Remarkably, raltegravir used up to 1 mM did not alter calcein accumulation in any cell type confirming a poor/null inhibitory effect on P-gp efflux activity.

Overall, these radiolabelled, and fluorescent-based experiments, demonstrate HIV-1 PIs/raltegravir drug−drug interactions at the P-gp level and confirms raltegravir as a null P-gp inhibitor *in vitro*.

Raltegravir intracellular levels are significantly reduced in primary CD3+CD4+P-gp^{high} cells

After assessing the substrate specificity of P-gp for raltegravir in the lymphoblastoid CD4+ T cell model CEM cells, we aimed to test raltegravir intracellular accumulation in primary CD4+ T cells. To do so, we used the P-gp-specific fluorescent dye Rho123 to distinguish between CD4+ T cell subsets with differential activity of P-gp in PBMCs from healthy donors. As shown in Figure 3(a), gating in CD3+CD4+ T cells, we could distinguish between two subpopulations based on Rho123 fluorescence: the Rho123 very low (P-gp activity high; P-gp^{high}) and Rho123 high (P-gp activity low; P-gp^{low}). Thus, we sorted these two populations to perform drug cellular accumulation experiments with
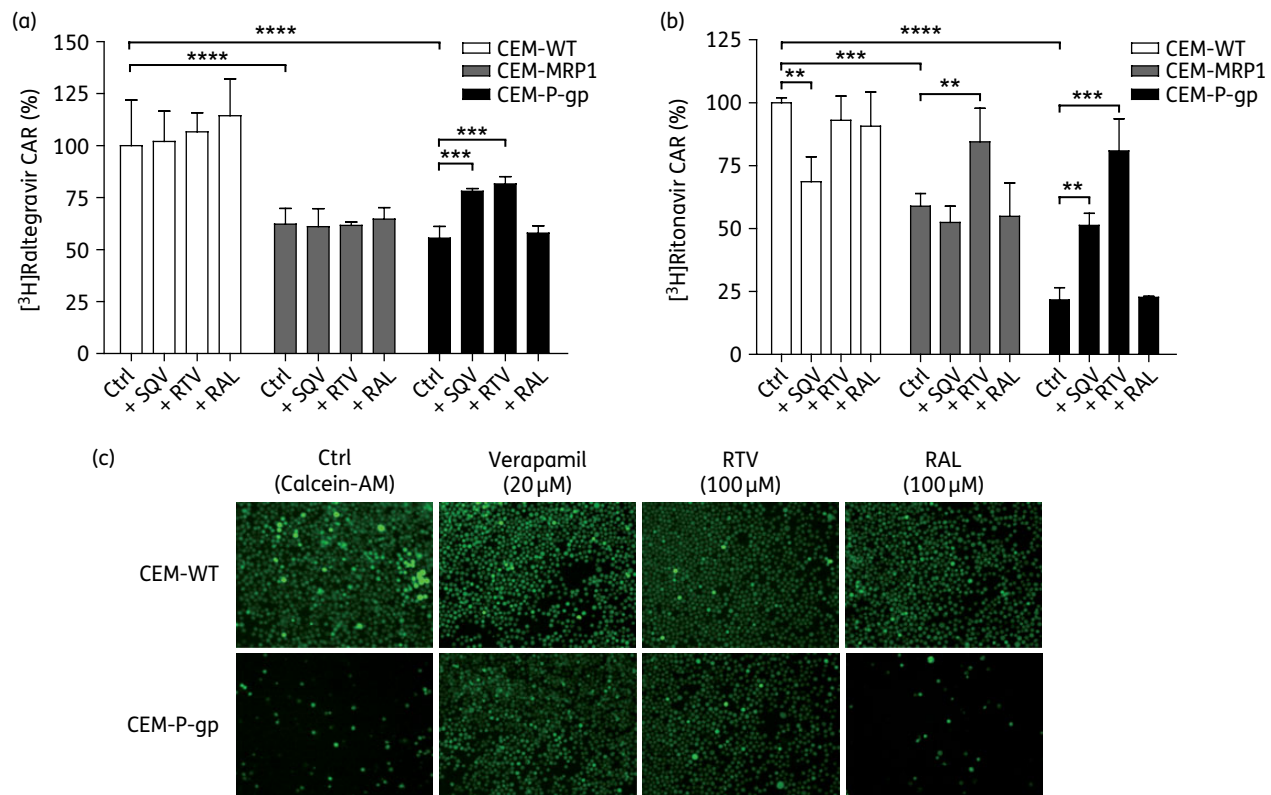
Figure 2. Inhibition of raltegravir and model substrate ritonavir efflux by HIV-1 PIs saquinavir and ritonavir. (a) [^{3}H]Raltegravir (1 μM; 0.5 μCi/mL) was incubated for 30 min in CEM cells in the absence (control) or presence of 100 μM saquinavir, ritonavir or raltegravir in the extracellular site and CAR was determined. (b) [^{3}H]Ritonavir (1 μM; 1 μCi/mL) was incubated for 30 min with CEM cells in the absence (control) or presence of 100 μM saquinavir, ritonavir or raltegravir. Results are expressed as the percentage of CAR normalized to CEM-WT cells (control cells) and represent the mean ± SEM of three independent experiments performed in duplicate. Statistical significance between each control CEM-WT, CEM-MRP1 and CEM-P-gp and between control and PI or raltegravir treatment was assessed by paired *t*-test (**$P < 0.01$; ***$P < 0.001$). (c) *Cis*-inhibition of the fluorescent substrate calcein in CEM-WT and CEM-P-gp cells. Calcein-AM (0.25 μM) was incubated for 20 min at 37°C in CEM-WT or CEM-P-gp in the absence or presence of 20 μM verapamil (broad-spectrum efflux transporter inhibitor), 100 μM ritonavir or 100 μM raltegravir. Intracellular calcein fluorescence was assessed in live culture cells by fluorescence microscopy. Ctrl, control; RAL, raltegravir; RTV, ritonavir; SQV, saquinavir. This figure appears in colour in the online version of *JAC* and in black and white in the print version of *JAC*.

[^{3}H]raltegravir (30 min) (Figure 3b). In accordance with our results in CEM cells, CD3+CD4+P-gp^{high} cells effluxed raltegravir more efficiently than P-gp^{low} cells, accumulating from 30% to 50% (38.4% ± 9.6%) less intracellular raltegravir ($P = 0.0097$). Most importantly, when incubating the cells with the P-gp-specific inhibitor XR9051, we could significantly reverse this effect ($P = 0.017$). Furthermore, when using total unsorted PBMCs, we found a difference in intracellular levels of [^{3}H]raltegravir versus CD4+P-gp^{low} cells ($P = 0.034$), not only due to the presence of a significant amount of CD8+ T cells and NK cells, known to have really high P-gp activity,[26] but also to the small fraction of CD4+ T cells P-gp[high]. Of note, the decrease in raltegravir accumulation could also be reversed by XR9051 inhibitor ($P = 0.017$). This is the first demonstration of raltegravir efflux via P-gp in primary CD4+ T cells.

HIV-1 infection increases P-gp expression in vitro and P-gp^{high} cells sustain higher HIV-1 infection rates

Next, we studied whether HIV-1 infection was capable of altering P-gp expression and/or activity. Thus, we assessed the effect of

HIV-1 infection on P-gp expression in PBMCs cultured in either IL-2 alone or in IL-2 plus PHA (Figure 4a). P-gp mRNA expression significantly increased from 1.7- to 2.4-fold when the cells were infected with HIV-1[NL4-3] (CXCR4-tropic strain) and cultured in IL-2 only, with the strongest effect found at moi 0.1. When cells were infected after 3 days activation in PHA, the increase in P-gp mRNA expression varied from 1.5- to 3.6-fold.

We also assessed P-gp activity by calcein efflux after PHA activation in three different primary samples from blood donors (Figure 4b). In CD4+ T lymphocytes, we found an overall dramatic decrease in calcein accumulation (red histogram) in accordance to a strong overall activation of P-gp activity. When using the P-gp-specific inhibitor XR9051 in non-stimulated CD4+, the activity of P-gp^{high} cells was remarkably inhibited seen as a drastic reduction in calcein efflux (peak between 10^1 and 10^2 in Figure 4b; see black arrows).

Finally, we also tested HIV-1 infection levels in primary CD3+CD4+P-gp[low] and P-gp[high] subsets. Surprisingly, after 6 days post-infection, P-gp^{high} cells showed a significantly higher level of intracellular HIV-1 p24[Gag] antigen. The effect was present in the three donors tested even though the infection levels were

Table 1. Calcein fluorescence ratio values normalized to CEM-WT (CEM-CCRF) untreated cells as found by flow cytometry analysis

Treatment	Fluorescence ratio (MFI treated/MFI mock cells)		
	CEM-WT	CEM-MRP1	CEM-P-gp
Untreated (mock)	1.00	0.181	0.018
Efflux inhibitors			
Ko143	0.77	**2.80**	**14.38**
verapamil	1.18	**5.34**	**40.12**
MK571	1.16	**2.53**	1.20
XR9051	0.94	0.90	**20.99**
PIs			
amprenavir	0.87	**3.49**	**47.53**
atazanavir	0.63	**2.54**	**47.97**
ritovanir	0.87	**5.00**	**65.41**
saquinavir	0.77	**3.94**	**37.94**
indinavir	1.28	2.11	2.21
lopinavir	0.60	**4.20**	**39.03**
NNRTIs			
efavirenz	0.94	**4.38**	**21.49**
nevirapine	0.92	1.23	2.02
INIs			
raltegravir 1 μM	0.77	1.13	1.04
raltegravir 10 μM	1.16	1.21	1.18
raltegravir 100 μM	1.18	1.31	1.35
raltegravir 1 mM	0.54^a	0.51^a	2.03

Values >2.50 are highlighted in bold.
^{a}Decrease in fluorescence ratio due to low raltegravir solubility at 1 mM.

very different (particularly in donor 3). The p24^{Gag} levels increased dramatically at days 9, 11 and 13 post-infection (particularly in donors 2 and 3) in P-gp^{high} cells, whereas P-gp^{low} cells showed a very slight or null increase. These data suggest that P-gp^{high} cells are a more activated subtype of CD4+ T cells that can sustain a higher HIV-1 replication rate. Overall, these experiments suggest P-gp activation (by both protein activity and mRNA expression) after HIV-1 infection and, surprisingly, a differential infection effect on CD4+P-gp^{high} and P-gp^{low} cells.

Correlation between P-gp activity and HIV-1 viral load in CD4+ T cell subsets

We then tested whether different CD4+ T cell subsets show correlation between P-gp activity and HIV-1 viral load, by analysing the percentage of total P-gp active cells of specific T cell subsets versus viral load (in log$_{10}$ copies of HIV-1 RNA per mL) of each HIV-1-infected subject (see the Materials and methods section). As shown in Figure 5(a–c), CD4+ T cells ($r=0.505$, $P=0.033$), CD4+CCR5+ ($r=0.538$, $P=0.021$) and double positive CCR5+CXCR4+ cells ($r=0.571$, $P=0.013$) showed a positive correlation between the increase in HIV-1 viral load and percentage of P-gp active cells. The most significant correlation between HIV-1 viral load and P-gp active cells was found within the

memory CD4+ T cell subset (defined as CD4+CD45RA−) ($r=0.792$, $P<0.0001$) (Figure 5d). Similar correlations were also found for central memory CD4+ T cells (T$_{CM}$, defined as CD4+CD45RA−CD27+CCR7+) ($r=0.572$, $P=0.013$) (Figure 5e) and transitional memory CD4+ T cells (T$_{TM}$, defined as CD4+CD45RA−CD27+CCR7−) ($r=0.536$, $P=0.022$) (Figure 5f). As hypothesized, both CD4+ T cells and memory CD4+ T cells, including some of their subsets showed a significant correlation between HIV-1 viral load in plasma and P-gp activity. This important finding suggests HIV-1 cellular activation as a key factor in modulating P-gp efflux activity.

Discussion

Experiments performed in our CD4+ T cell models confirmed an efflux transport of raltegravir by P-gp and a significant inhibition with the P-gp-specific blocker XR9051 as previously reported using different P-gp inhibitors.[29,30] In accordance with these previous reports, raltegravir seemed a relatively 'poor' substrate of P-gp in comparison with ritonavir, an HIV PI used as a control substrate (Figure 1b and c). However, the transporter could still be relevant *in vivo* and influence the pharmacokinetic/pharmacodynamic relationship or the drug clinical response. Moreover, Moss *et al.*[30] described reduced HIV PI uptake in CEM-MRP1 and CEM-P-gp versus CEM-WT cells, but their measurements started at 1 min, when, according to our measurements (Figure S1), the linear uptake phase is already ended. Thus, the contribution of uptake transport in the experiments performed at longer time points than 5 min is residual.

In parallel we ruled out MRP1 as an efflux transporter for raltegravir and confirmed previously shown null inhibition of P-gp function by raltegravir.[29,30] This, along with evidence showing that ritonavir and other HIV-1 PIs efficiently inhibited its own and raltegravir efflux, suggests that P-gp has a translocation binding site for raltegravir and a spatially separated site, where other drugs could act as allosteric inhibitors.[37] Ritonavir could be competing for the transport in the translocation site or allosterically inhibiting its own efflux, binding to a different (extra- or intracellular) site of P-gp. Of note, as for raltegravir, many P-gp substrates are not suitable inhibitors of the ATP-efflux transporter[38] and the occurrence of binding sites with different functional properties has been also reported for the SLC superfamily of transporters (e.g. OCT1).[39,40]

This study also showed that most HIV-1 PIs (except for indinavir) inhibited both MRP1 and P-gp function. The latter phenomenon would be relevant for raltegravir drug disposition and pharmacokinetics as raltegravir is usually co-administered with PIs, particularly darunavir or atazanavir, both 'boosted' with ritonavir.[1] However, atazanavir increases raltegravir systemic exposure by inhibiting its main metabolizing enzyme UDP-glucuronosyltransferase 1 family polypeptide 1A (UGT1A1).[41] On the other hand, darunavir has been recently shown to inhibit P-gp activity *in vitro*;[42] thus, if affecting the pump *in vivo*, its co-administration with raltegravir would favour its persistence in certain cell subsets with high P-gp activity. In radiolabelled experiments with CEM-P-gp cells in the presence of saquinavir and ritonavir, raltegravir showed 20%–40% higher intracellular accumulation. Assuming that plasma concentrations of PIs in patients are sufficient to inhibit P-gp activity, favourable drug–drug interactions could be occurring at this level. Some previous
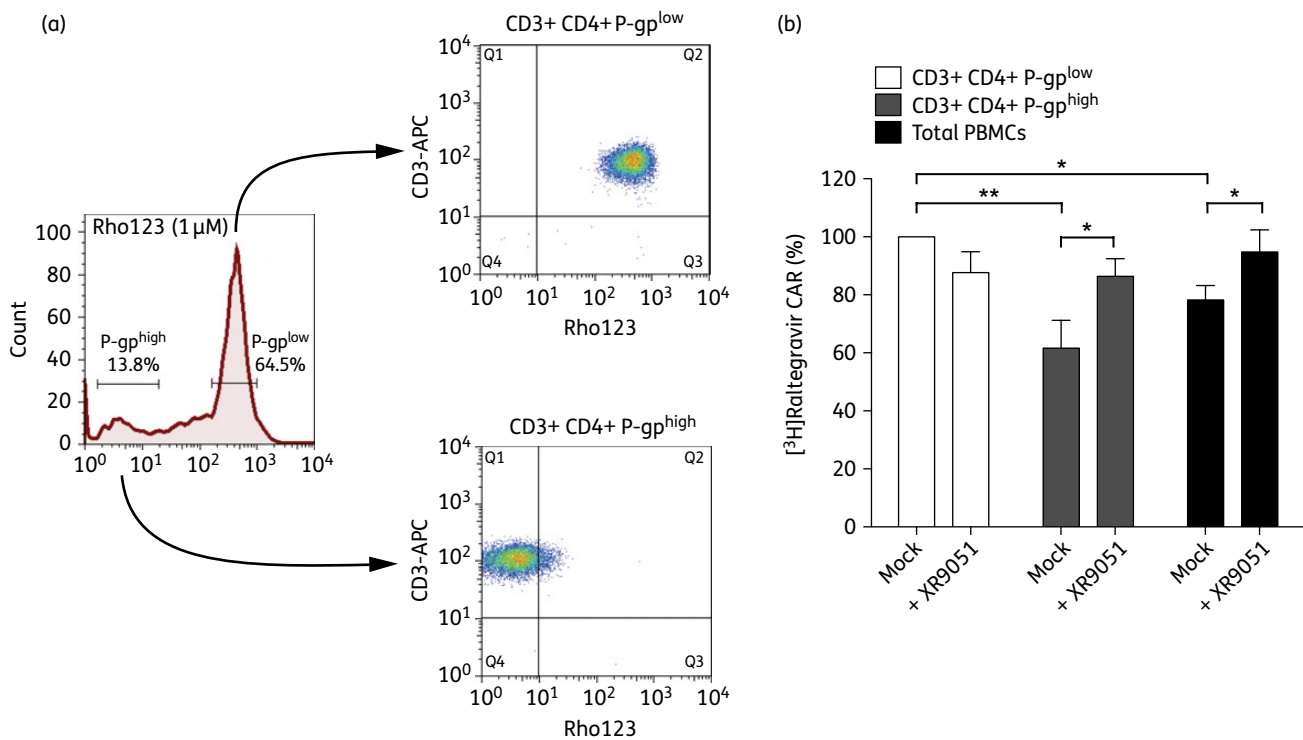
Figure 3. Raltegravir intracellular accumulation analysis of CD3+CD4+P-gp^high and P-gp^low populations. (a) After Rho123 incubation (1 μM, 20 min, 37°C), PBMCs were put in culture (complete medium) during 2 h to let the dye be effluxed and then stained with anti-CD3-APC and anti-CD4-PerCP antibodies. CD3+CD4+ T cells were sorted based on their Rho123 staining: P-gp^high (Rho123 very low) and P-gp^low (Rho123 high). Cells were directly used in subsequent [³H]raltegravir accumulation assays. (b) CD3+CD4+P-gp^high and CD3+CD4+P-gp^low cells were incubated in transport medium with 1 μM (1 μCi/mL) [³H]raltegravir in the absence (mock) or presence of the P-gp-specific inhibitor XR9051 (1 μM). Unsorted (total) PBMCs were used as control of viability and transport, considering that they contain CD8+ T cells, NK and monocytes. The results represent the mean ± SEM of five independent experiments (each with a different blood donor) performed in duplicate. Statistical significance was assessed by paired *t*-test (*$P < 0.05$; **$P < 0.01$; $n = 5$). This figure appears in colour in the online version of *JAC* and in black and white in the print version of *JAC*.

pharmacokinetic reports only indicate remarkable interactions between atazanavir[41] and raltegravir, but no other PIs.[43,44] However, the lack of fine experimental techniques to detect efficiently the intracellular drug levels in different blood cell subsets may mask relevant interactions[45–47] responsible for the high variability in raltegravir levels in patients.[19,20] Most importantly, subsets of primary CD3+CD4+ cells with remarkable different P-gp activity (namely P-gp^high and P-gp^low; see Figure 3) showed variable intracellular raltegravir concentrations. The extracellular treatment of the CD4+P-gp^high with the P-gp-specific blocker XR9051, significantly increased the intracellular accumulation of raltegravir, indicating that P-gp is important for its intracellular disposition in primary CD4+ T cells. In addition, we assessed the possible contribution of BCRP1 (another relevant ABC transporter), which has been reported to be expressed with high inter-individual variability on circulating CD4+ T cells.[48] Compared with P-gp, we found negligible *ABCG2* mRNA and BCRP1 protein expression in CEM-MRP1, CEM-P-gp, freshly isolated PBMCs and primary CD4+ T cells (Figure S3), as well as a null inhibition of calcein accumulation in the presence of low doses (<1 μM) of Ko143 in the latter cells (data not shown). Whether the reduction in raltegravir levels in these cells could be affecting drug activity and HIV-1 suppression *in vivo* is something that needs further investigation. However, we hypothesize that long-lasting CD4+ T cell subsets (such as CD4+

T_CM cells) with high P-gp activity would be partially refractory to raltegravir (or other HIV-1 drugs that are substrates for P-gp) and could represent HIV-1 cellular reservoirs *in vivo*. Recently, a small proportion of CD4+ memory T cells with stem-cell like properties (termed CD4+ T_SCM) have been described as HIV-1 long-term reservoirs; this subset can harbour high levels of HIV-1 DNA and significantly contribute to HIV-1 persistence.[14] In accordance, it is well known that haematopoietic stem cells have high levels of P-gp[49] and other efflux pumps (i.e. BCRP). Thus, in addition to containing fewer HIV-1 restriction factors,[14] CD4+ stem cell-like memory T cells (T_SCM) may also be more refractory to the HAART regimen due to higher levels or activity of P-gp or other efflux transporters. Interestingly, it has also been suggested that transcriptionally quiescent thymocytes (CD3^highCD27+) and NK cells, showing high P-gp activity, may be a pharmacological sanctuary site for HIV-1.[34,50]

We then addressed the question of whether the virus and cellular activation influences P-gp activity by infecting CD4+ T cells *in vitro*, in the presence of IL-2 or IL-2/PHA. HIV-1 infection significantly increased mRNA expression of P-gp, and the activation of CD4+ T cells by PHA showed increased P-gp activity, an effect that could be reversed by the P-gp-specific inhibitor XR9051, in unstimulated primary CD4+ T cells. In studies done in human and rat astrocytes, IL-6 secretion after HIV-1 glycoprotein
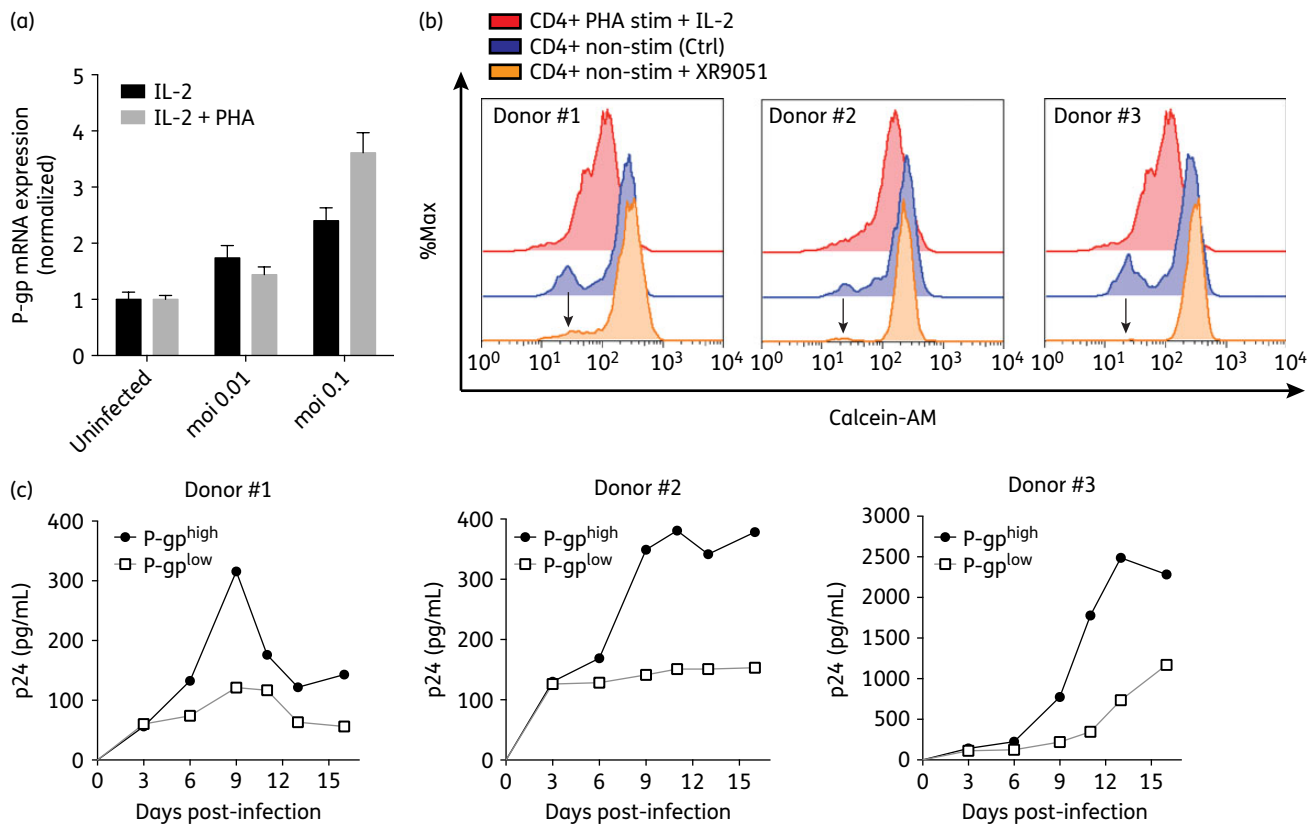
Figure 4. Effect of HIV-1 infection and cellular activation on P-gp expression and activity. (a) P-gp mRNA levels were assessed by quantitative real-time PCR in PBMCs (pooled from three donors) cultured in IL-2 or IL-2+PHA after infection with HIV-1$_{NL4-3}$ at two different moi (0.01 and 0.1) for 48 h. Results represent the average of two independent experiments with three pooled donors each performed in triplicate. (b) Calcein-AM accumulation in CD3+CD4+ sorted cells from three independent donors was analysed by flow cytometry in non-stimulated cells, PHA-stimulated cells and non-stimulated cells treated with the P-gp inhibitor XR9051 (1 μM, during the 2 h efflux time) to decipher the effect of cellular activation on P-gp activity. Results show three independent representative donors of a total of five donors; thin black arrows indicate the reduction in calcein efflux (10^1–10^2 peak disappearance). (c) HIV-1$_{NL4-3}$ infection (moi=0.1) in CD3+CD4+P-gp^{high} and P-gp^{low} cells from three independent donors was followed up to 16 days post-infection by antigen p24^{Gag} ELISA. Ctrl, control; stim, stimulated. This figure appears in colour in the online version of *JAC* and in black and white in the print version of *JAC*.

gp120 treatment decreases the P-gp expression and activity,[51,52] whereas only TNF-α increases P-gp and MRP1 expression, but not IL-1β or IL-6, for the latter transporter.[52,53] More importantly, we found that sorted CD4+P-gp^{high} cells achieved higher levels of HIV-1 replication (by p24^{Gag} antigen) than P-gp^{low} cells, most probably due to a higher activation rate of these cells. The same effect was confirmed in our CD4+ T lymphoblastoid cell models (CEM-P-gp versus CEM-WT). In accordance, previous findings demonstrated a more prominent depletion of HIV-1 infection on CD4+CCR5+ with high expression of P-gp[26] contrary to the hypothesis that high P-gp expression can confer a protective effect against HIV-1 infection by steric hindrance or other physicochemical properties.[36,52] In their work, Valentin *et al.*[26] described that 15%–33% of *in vitro* HIV-1-infected PBMCs have high P-gp activity, but they did not compare HIV replication rates between CD4+P-gp^{high} and P-gp^{low} subsets. Furthermore, they found a decrease in CD4+CCR5+P-gp^{high} cells in HIV-1-infected individuals versus HIV-1 seronegative donors. In our patient cohort, we observed a similar trend for CD4+CXCR4+, where the percentage of P-gp^{high} was decreased

in HIV-1-infected subjects versus HIV-1 seronegative individuals and in high viraemic (>100 000 copies/mL) versus low viraemic (<30 000 copies/mL) HIV-1-infected patients (data not shown). This suggests the need for a high viral presence in the blood to deplete selectively the CD4+P-gp^{high} cell populations. Importantly, high viraemic HIV-1-infected subjects show lower raltegravir rate success than low viraemic subjects in both naïve[16] and treatment-experienced patients[54] with drug-resistant HIV infection. Furthermore, the nucleoside-sparing regimen of darunavir/ritonavir plus raltegravir showed a higher rate of virological failure and integrase resistance in high viraemic patients.[55] Thus, we should consider the long-term survival of the residual percentage of CD4+P-gp^{high} cells (expressing HIV-1 co-receptors) as a putative cause for HIV-1 latency, drug resistance and virological failure as they would represent a cellular reservoir.

Most importantly, we found a significant correlation between HIV-1 viral load and P-gp activity [considering total P-gp active cells as reported by Haraguchi *et al.*,[34] not only the P-gp very active (P-gp^{high}) population] in different subsets of CD4+ T cells:
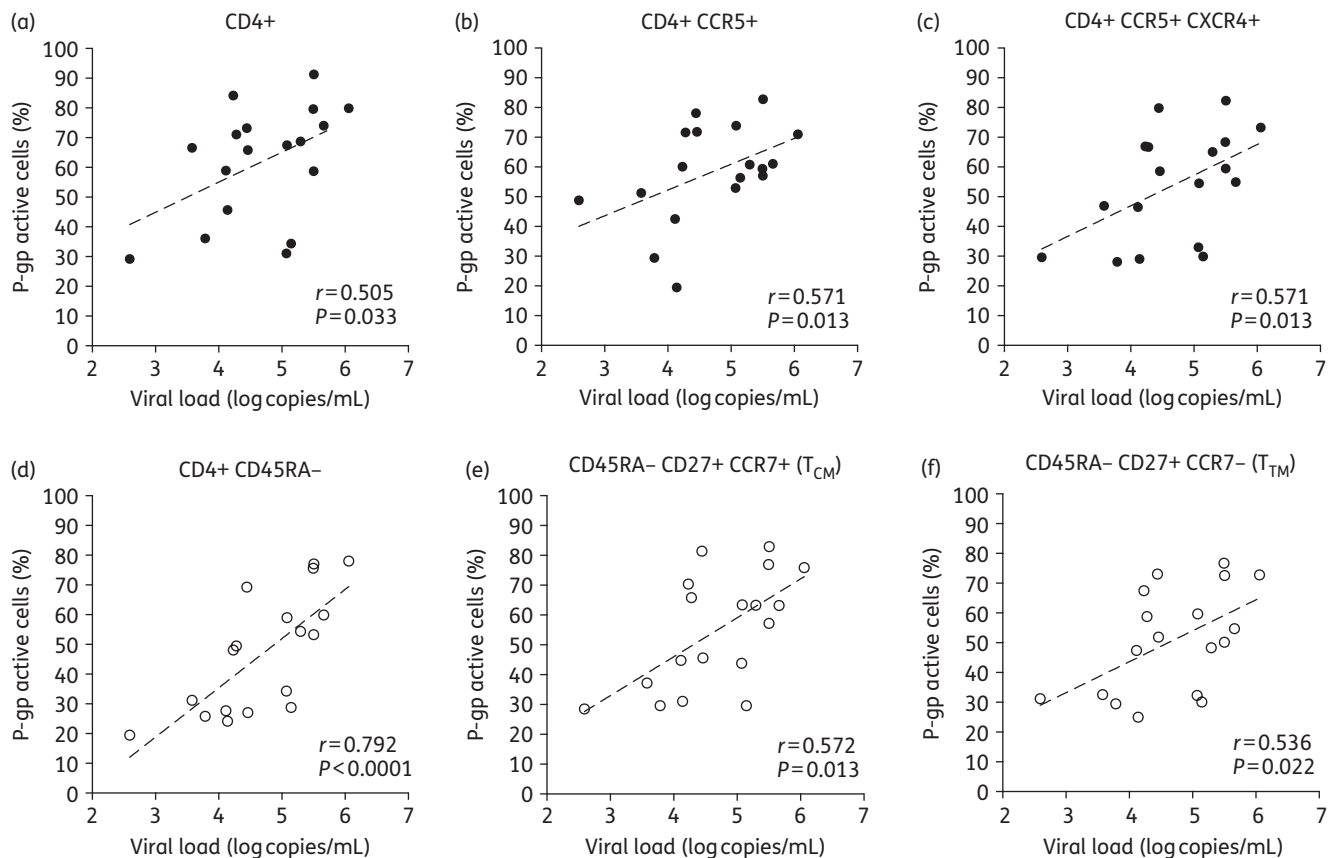
Figure 5. P-gp activity correlation with plasma viral load in different CD4+ subsets in HIV-1-infected subjects. HIV-1-infected blood samples were processed by Ficoll-Paque to obtain the PBMC fraction and loaded with Rho123. After 2 h of efflux time, cells were stained with two panels of antibodies (plus CD3-APC and CD4-PerCP, present in both panels): (i) HIV-1 co-receptors, CXCR4 and CCR5; and (ii) naive/memory populations (CD45RA, CD27, CCR7). CD3+CD4+, CD4+CCR5+ and double positive (CD4+CCR5+CXCR4+) populations and their correlations with plasma viral load (HIV-1 RNA log copies/mL) are shown in (a), (b) and (c), respectively. (d), (e) and (f) show CD4+CD45RA− (memory T cells), CD45RA−CD27+CCR7+ (T central memory, T_{CM}) and CD45RA−CD27+CCR7− (T transitional memory, T_{TM}) correlations. Statistical analyses were performed by Spearman correlations (*r*) of percentage of P-gp active cells versus viral load. Statistically significant *P* values <0.05 are shown together with *r* values.

the higher the viral load, the higher the P-gp activity in CD4+ T cells. The greatest correlation was found in the whole population of memory T cells (CD3+CD4+CD45RA−) (Figure 5d; $r=0.792$, $P<0.0001$). Of note, central memory (T_{CM})—very long-lived cells—and transitional memory T cells (T_{TM}) showed a correlation between increase in viral load and P-gp activity. Other groups have studied ABC transporters mRNA expression or P-gp and MRP activity in infected patients, but the results are controversial, mostly due to different methods employed and the heterogeneity in the populations and drug treatments compared.[35,46,47,56,57] Of note, Turriziani *et al.*[57] found a higher mRNA expression of the genes encoding for P-gp, MRP1, MRP4 and MRP5 in HIV-positive patients in comparison with healthy donors. In contrast, Meaden *et al.*[47] found a decrease in membrane P-gp expression by flow cytometry in PBMCs of HIV-1-positive individuals (17 of a total of 21, on HAART). In our study, the increase in P-gp activity in the presence of high viral load in HIV-1-infected subjects, suggests an important phenomenon *in vivo*: a higher virus presence in blood would mean a higher T cell activation and a higher efflux transport mechanism of P-gp. Overall, HIV-1-associated cell activation increases P-gp activity, but, at the same time, P-gp^high cells

are also more susceptible to HIV-1 infection, to HIV-related apoptosis and more refractory to PIs and raltegravir. Thus, the percentage of CD4+P-gp^high subsets that would be infected and would survive with the integrated virus, could represent a population with persistent HIV-1 and a threat for HIV-1 eradication as previously suggested for mature thymocytes[34] and demonstrated for NK cells[50] and stem-cell like CD4+ (T_{SCM}) cells.[14] Better characterization of the different P-gp^high T cell subsets and deciphering if the novel stem cell-like CD4+ (T_{SCM}) cells have high levels of P-gp (or other ABC transporters) would help to find ways to target it more efficiently, increasing raltegravir and PI clinical outcome and minimizing HIV-1 persistence.

Overall, we have demonstrated an important role of P-gp for raltegravir efflux in primary CD4+ cells and the *in vivo* effect of HIV-1 on the activity of the transporter. Higher levels of virus in the blood increase P-gp efflux and might decrease drug regimen success. However, the CD4+P-gp^high cells are also more readily depleted by HIV-1. Thus, HIV-1 plasma levels and the clearance of CD4+P-gp^high subsets might influence treatment efficacy, particularly when systemic exposure to raltegravir is not warranted.

JAC

Supplementary data

Supplementary methods, Figures S1 to S3 are available as Supplementary data at *JAC* Online (http://jac.oxfordjournals.org/).

References

1 Gunthard HF, Aberg JA, Eron JJ et al. Antiretroviral treatment of adult HIV infection: 2014 recommendations of the International Antiviral Society-USA Panel. JAMA 2014; **312**: 410–25.

2 Lennox JL, Dejesus E, Berger D et al. Raltegravir versus Efavirenz regimens in treatment-naive HIV-1-infected patients: 96-week efficacy, durability, subgroup, safety, and metabolic analyses. J Acquir Immune Defic Syndr 2010; **55**: 39–48.

3 Lennox JL, Dejesus E, Lazzarin A et al. Safety and efficacy of raltegravir-based versus efavirenz-based combination therapy in treatment-naive patients with HIV-1 infection: a multicentre, double-blind randomised controlled trial. Lancet 2009; **374**: 796–806.

4 Markowitz M, Morales-Ramirez JO, Nguyen BY et al. Antiretroviral activity, pharmacokinetics, and tolerability of MK-0518, a novel inhibitor of HIV-1 integrase, dosed as monotherapy for 10 days in treatment-naive HIV-1-infected individuals. J Acquir Immune Defic Syndr 2006; **43**: 509–15.

5 Markowitz M, Nguyen BY, Gotuzzo E et al. Rapid and durable antiretroviral effect of the HIV-1 Integrase inhibitor raltegravir as part of combination therapy in treatment-naive patients with HIV-1 infection: results of a 48-week controlled study. J Acquir Immune Defic Syndr 2007; **46**: 125–33.

6 Cooper DA, Steigbigel RT, Gatell JM et al. Subgroup and resistance analyses of raltegravir for resistant HIV-1 infection. N Engl J Med 2008; **359**: 355–65.

7 Gatell JM, Katlama C, Grinsztejn B et al. Long-term efficacy and safety of the HIV integrase inhibitor raltegravir in patients with limited treatment options in a Phase II study. J Acquir Immune Defic Syndr 2010; **53**: 456–63.

8 Steigbigel RT, Cooper DA, Kumar PN et al. Raltegravir with optimized background therapy for resistant HIV-1 infection. N Engl J Med 2008; **359**: 339–54.

9 Lee FJ, Carr A. Tolerability of HIV integrase inhibitors. Curr Opin HIV AIDS 2012; **7**: 422–8.

10 Jung N, Taubert D. Organic cation transporters and their roles in anti-retroviral drug disposition. Expert Opin Drug Metab Toxicol 2009; **5**: 773–87.

11 Minuesa G, Huber-Ruano I, Pastor-Anglada M et al. Drug uptake transporters in antiretroviral therapy. Pharmacol Ther 2011; **132**: 268–79.

12 Pastor-Anglada M, Cano-Soldado P, Molina-Arcas M et al. Cell entry and export of nucleoside analogues. Virus Res 2005; **107**: 151–64.

13 Cianfriglia M, Dupuis ML, Molinari A et al. HIV-1 integrase inhibitors are substrates for the multidrug transporter MDR1-P-glycoprotein. Retrovirology 2007; **4**: 17.

14 Buzon MJ, Sun H, Li C et al. HIV-1 persistence in CD4+ T cells with stem cell-like properties. Nat Med 2014; **20**: 139–42.

15 Arab-Alameddine M, Fayet-Mello A, Lubomirov R et al. Population pharmacokinetic analysis and pharmacogenetics of raltegravir in HIV-positive and healthy individuals. Antimicrob Agents Chemother 2012; **56**: 2959–66.

16 Eron JJ Jr, Rockstroh JK, Reynes J et al. Raltegravir once daily or twice daily in previously untreated patients with HIV-1: a randomised, active-controlled, phase 3 non-inferiority trial. Lancet Infect Dis 2011; **11**: 907–15.

17 Rizk ML, Hang Y, Luo WL et al. Pharmacokinetics and pharmacodynamics of once-daily versus twice-daily raltegravir in treatment-naive HIV-infected patients. Antimicrob Agents Chemother 2012; **56**: 3101–6.

18 Miller M. Analysis of resistance to the HIV-1 integrase inhibitor raltegravir: results from the Benchmark 1 and 2. In: Abstracts of the Forty-eighth Interscience Conference on Antimicrobial Agents and Chemotherapy, Washington, DC, 2008. Abstract H-898. American Society for Microbiology, Washington, DC, USA.

19 Fayet-Mello A, Buclin T, Franc C et al. Cell disposition of raltegravir and newer antiretrovirals in HIV-infected patients: high inter-individual variability in raltegravir cellular penetration. J Antimicrob Chemother 2011; **66**: 1573–81.

20 Cattaneo D, Gervasoni C, Meraviglia P et al. Inter- and intra-patient variability of raltegravir pharmacokinetics in HIV-1-infected subjects. J Antimicrob Chemother 2012; **67**: 460–4.

21 Lee CG, Gottesman MM, Cardarelli CO et al. HIV-1 protease inhibitors are substrates for the MDR1 multidrug transporter. Biochemistry 1998; **37**: 3594–601.

22 Olson DP, Scadden DT, D'Aquila RT et al. The protease inhibitor ritonavir inhibits the functional activity of the multidrug resistance related-protein 1 (MRP-1). AIDS 2002; **16**: 1743–7.

23 Profit L, Eagling VA, Back DJ. Modulation of P-glycoprotein function in human lymphocytes and Caco-2 cell monolayers by HIV-1 protease inhibitors. AIDS 1999; **13**: 1623–7.

24 Janneh O, Chandler B, Hartkoorn R et al. Intracellular accumulation of efavirenz and nevirapine is independent of P-glycoprotein activity in cultured CD4 T cells and primary human lymphocytes. J Antimicrob Chemother 2009; **64**: 1002–7.

25 Jones K, Bray PG, Khoo SH et al. P-Glycoprotein and transporter MRP1 reduce HIV protease inhibitor uptake in CD4 cells: potential for accelerated viral drug resistance? AIDS 2001; **15**: 1353–8.

26 Valentin A, Morrow M, Poirier RH et al. Identification of a potential pharmacological sanctuary for HIV type 1 in a fraction of CD4+ primary cells. AIDS Res Hum Retroviruses 2010; **26**: 79–88.

27 Dupuis ML, Ascione A, Palmisano L *et al*. Raltegravir does not revert efflux activity of MDR1-P-glycoprotein in human MDR cells. *BMC Pharmacol Toxicol* 2013; **14**: 47.

28 Hashiguchi Y, Hamada A, Shinohara T *et al*. Role of P-glycoprotein in the efflux of raltegravir from human intestinal cells and CD4+ T-cells as an interaction target for anti-HIV agents. *Biochem Biophys Res Commun* 2013; **439**: 221–7.

29 Hoque MT, Kis O, De Rosa MF *et al*. Raltegravir permeability across blood-tissue barriers and the potential role of drug efflux transporters. *Antimicrob Agents Chemother* 2015; **59**: 2572–82.

30 Moss DM, Kwan WS, Liptrott NJ *et al*. Raltegravir is a substrate for SLC22A6: a putative mechanism for the interaction between raltegravir and tenofovir. *Antimicrob Agents Chemother* 2011; **55**: 879–87.

31 Beck WT, Mueller TJ, Tanzer LR. Altered surface membrane glycoproteins in Vinca alkaloid-resistant human leukemic lymphoblasts. *Cancer Res* 1979; **39**: 2070–6.

32 Davey MW, Hargrave RM, Davey RA. Comparison of drug accumulation in P-glycoprotein-expressing and MRP-expressing human leukaemia cells. *Leuk Res* 1996; **20**: 657–64.

33 Janneh O, Owen A, Chandler B *et al*. Modulation of the intracellular accumulation of saquinavir in peripheral blood mononuclear cells by inhibitors of MRP1, MRP2, P-gp and BCRP. *AIDS* 2005; **19**: 2097–102.

34 Haraguchi S, Ho SK, Morrow M *et al*. Developmental regulation of P-glycoprotein activity within thymocytes results in increased anti-HIV protease inhibitor activity. *J Leuk Biol* 2011; **90**: 653–60.

35 Lucia MB, Cauda R, Landay AL *et al*. Transmembrane P-glycoprotein (P-gp/P-170) in HIV infection: analysis of lymphocyte surface expression and drug-unrelated function. *AIDS Res Hum Retroviruses* 1995; **11**: 893–901.

36 Speck RR, Yu XF, Hildreth J *et al*. Differential effects of p-glycoprotein and multidrug resistance protein-1 on productive human immunodeficiency virus infection. *J Infect Dis* 2002; **186**: 332–40.

37 Martin C, Berridge G, Higgins CF *et al*. Communication between multiple drug binding sites on P-glycoprotein. *Mol Pharmacol* 2000; **58**: 624–32.

38 Barecki-Roach M, Wang EJ, Johnson WW. Many P-glycoprotein substrates do not inhibit the transport process across cell membranes. *Xenobiotica* 2003; **33**: 131–40.

39 Ahlin G, Chen L, Lazorova L *et al*. Genotype-dependent effects of inhibitors of the organic cation transporter, OCT1: predictions of metformin interactions. *Pharmacogenomics J* 2011; **11**: 400–11.

40 Bachmakov I, Glaeser H, Fromm MF *et al*. Interaction of oral antidiabetic drugs with hepatic uptake transporters: focus on organic anion transporting polypeptides and organic cation transporter 1. *Diabetes* 2008; **57**: 1463–9.

41 Neely M, Decosterd L, Fayet A *et al*. Pharmacokinetics and pharmacogenomics of once-daily raltegravir and atazanavir in healthy volunteers. *Antimicrob Agents Chemother* 2010; **54**: 4619–25.

42 Tempestilli M, Gentilotti E, Tommasi C *et al*. Determination of P-glycoprotein surface expression and functional ability after in vitro treatment with darunavir or raltegravir in lymphocytes of healthy donors. *Int Immunopharmacol* 2013; **16**: 492–7.

43 Iwamoto M, Wenning LA, Petry AS *et al*. Minimal effects of ritonavir and efavirenz on the pharmacokinetics of raltegravir. *Antimicrob Agents Chemother* 2008; **52**: 4338–43.

44 Jackson A, Watson V, Back D *et al*. Plasma and intracellular pharmacokinetics of darunavir/ritonavir once daily and raltegravir once and twice daily in HIV-infected individuals. *J Acquir Immune Defic Syndr* 2011; **58**: 450–7.

45 Nies AT, Koepsell H, Damme K *et al*. Organic cation transporters (OCTs, MATEs), in vitro and in vivo evidence for the importance in drug therapy. *Handb Exp Pharmacol* 2011; **201**: 105–67.

46 Andreana A, Aggarwal S, Gollapudi S *et al*. Abnormal expression of a 170-kilodalton P-glycoprotein encoded by MDR1 gene, a metabolically active efflux pump, in CD4+ and CD8+ T cells from patients with human immunodeficiency virus type 1 infection. *AIDS Res Hum Retroviruses* 1996; **12**: 1457–62.

47 Meaden ER, Hoggard PG, Maher B *et al*. Expression of P-glycoprotein and multidrug resistance-associated protein in healthy volunteers and HIV-infected patients. *AIDS Res Hum Retroviruses* 2001; **17**, 1329–32.

48 Zhang J-C, Deng Z-Y, Wang Y *et al*. Expression of breast cancer resistance protein in peripheral T cell subsets from HIV-1-infected patients with antiretroviral therapy. *Mol Med Reports* 2014; **10**: 939–46.

49 Chaudhary PM, Roninson IB. Expression and activity of P-glycoprotein, a multidrug efflux pump, in human hematopoietic stem cells. *Cell* 1991; **66**: 85–94.

50 Valentin A, Rosati M, Patenaude DJ *et al*. Persistent HIV-1 infection of natural killer cells in patients receiving highly active antiretroviral therapy. *Proc Natl Acad Sci USA* 2002; **99**: 7015–20.

51 Ashraf T, Ronaldson PT, Persidsky Y *et al*. Regulation of P-glycoprotein by human immunodeficiency virus-1 in primary cultures of human fetal astrocytes. *J Neurosci Res* 2011; **89**: 1773–82.

52 Ronaldson PT, Bendayan R. HIV-1 viral envelope glycoprotein gp120 triggers an inflammatory response in cultured rat astrocytes and regulates the functional expression of P-glycoprotein. *Mol Pharmacol* 2006; **70**: 1087–98.

53 Ronaldson PT, Ashraf T, Bendayan R. Regulation of multidrug resistance protein 1 by tumor necrosis factor alpha in cultured glial cells: involvement of nuclear factor-kappaB and c-Jun N-terminal kinase signaling pathways. *Mol Pharmacol* 2010; **77**: 644–59.

54 Steigbigel RT, Cooper DA, Teppler H *et al*. Long-term efficacy and safety of Raltegravir combined with optimized background therapy in treatment-experienced patients with drug-resistant HIV infection: week 96 results of the BENCHMRK 1 and 2 Phase III trials. *Clin Infect* 2010; **50**: 605–12.

55 Taiwo B, Zheng L, Gallien S *et al*. Efficacy of a nucleoside-sparing regimen of darunavir/ritonavir plus raltegravir in treatment-naive HIV-1-infected patients (ACTG A5262). *AIDS* 2011; **25**: 2113–22.

56 Lucia MB, Savarino A, Straface E *et al*. Role of lymphocyte multidrug resistance protein 1 in HIV infection: expression, function, and consequences of inhibition. *J Acquir Immune Defic Syndr* 2005; **40**: 257–66.

57 Turriziani O, Gianotti N, Falasca F *et al*. Expression levels of MDR1, MRP1, MRP4, and MRP5 in peripheral blood mononuclear cells from HIV infected patients failing antiretroviral therapy. *J Med Virol* 2008; **80**: 766–71.